AD 716 960

AFCRL-71-0009

THREE-DIMENSIONAL SEISMIC RAY TRACING IN A LATERALLY HETEROGENEOUS SPHERICAL EARTH

by

Klaus H. Jacob

LAMONT-DOHERTY GEOLOGICAL OBSERVATORY OF COLUMBIA UNIVERSITY

Palisades, New York 10964

Contract No. F19628-68-C-0341

Project No. 8652

Task No. 865201

Work Unit No. 86520101

Scientific Report No. 13

January 4, 1971

Reprinted from the Journal of Geophysical Research, Vol. 75, No. 32, November 10, 1970, pages 6675-6689

This document has been approved for public release and sale; its distribution is unlimited.

Contract Monitor: Robert A. Gray

Terrestrial Sciences Laboratory

The views and conclusions contained in this document are those of the authors and should not be interpreted as necessarily representing the official policies, either expressed or implied, of the Advanced Research Projects Agency or the U. S. Government.

Sponsored by

Advanced Research Projects Agency

ARPA Order No. 292

Monitored by

AIR FORCE CAMBRIDGE RESEARCH LABORATORIES

AIR FORCE SYSTEMS COMMAND

UNITED STATES AIR FORCE

Bedford, Massachusetts 01730

DDC

RECEIVED

MAR 3 1971

C

NATIONAL TECHNICAL INFORMATION SERVICE

DISCLAIMER NOTICE

THIS DOCUMENT IS THE BEST QUALITY AVAILABLE.

COPY FURNISHED CONTAINED A SIGNIFICANT NUMBER OF PAGES WHICH DO NOT REPRODUCE LEGIBLY.

ARPA Order No. 292
Program Code No. 0F10
Effective Date of Contract .....1 August 1968
Contract Expiration Date .....30 June 1971
Principal Investigator and Phone No. .....Klaus H. Jacob, (914) 359-2900
Project Scientist or Engineer
and Phone No. .....Robert A. Gray (617) 861-3659

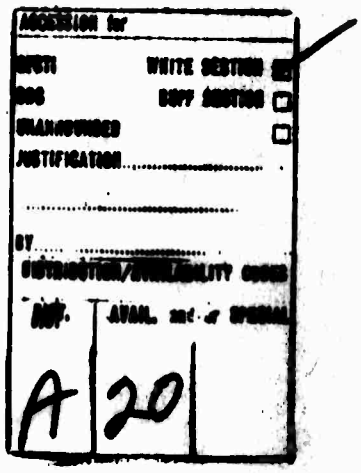

Qualified requesters may obtain additional copies from the Defense Documentation Center. All others should apply to the Clearinghouse for Federal Scientific and Technical Information.

AFCRL-71-0009

THREE-DIMENSIONAL SEISMIC RAY TRACING IN A LATERALLY HETEROGENEOUS SPHERICAL EARTH

by
Klaus H. Jacob
LAMONT-DOHERTY GEOLOGICAL OBSERVATORY OF COLUMBIA UNIVERSITY
Palisades, New York 10964

Contract No. F19628-68-C-0341
Project No. 8652
Task No. 865201
Work Unit No. 86520101

Scientific Report No. 13

January 4, 1971

Reprinted from the Journal of Geophysical Research, Vol. 75, No. 32,
November 10, 1970, pages 6675-6689

This document has been approved for public release
and sale; its distribution is unlimited.

Contract Monitor: Robert A. Gray
Terrestrial Sciences Laboratory

The views and conclusions contained in this document are those of the authors and should not be interpreted as necessarily representing the official policies, either expressed or implied, of the Advanced Research Projects Agency or the U. S. Government.

Sponsored by
Advanced Research Projects Agency
ARPA Order No. 292

Monitored by
AIR FORCE CAMBRIDGE RESEARCH LABORATORIES
AIR FORCE SYSTEMS COMMAND
UNITED STATES AIR FORCE
Bedford, Massachusetts 01730

ARPA Order No. 292
Program Code No. 0F10
Effective Date of Contract ..... 1 August 1968
Contract Expiration Date ..... 30 June 1971
Principal Investigator and Phone No. ..... Klaus H. Jacob, (914) 359-2900
Project Scientist or Engineer
and Phone No. ..... Robert A. Gray (617) 861-3659

Qualified requestors may obtain additional copies from the Defense Documentation Center. All others should apply to the Clearinghouse for Federal Scientific and Technical Information.

Three-Dimensional Seismic Ray Tracing in a Laterally Heterogeneous Spherical Earth[1]

KLAUS H. JACOB

Lamont-Doherty Geological Observatory of Columbia University
Palisades, New York 10964

Recent seismological studies suggest lateral inhomogeneities in P and S velocities of the mantle that are associated with slabs of mobile lithosphere descending into the mantle beneath island arcs. In special cases, travel times of P traversing such zones can differ by as much as 5 sec and of S by up to 10 sec from standard travel times. In addition, such zones are characterized by relatively low attenuation of S-wave energy compared with high attenuation in a broad zone on the landward side of the active volcanoes. To explain the observed anomalous travel times and attenuation phenomena, it is necessary to trace the path of body waves through laterally heterogeneous earth models. The technique of ray tracing developed here uses Fermat's principle to obtain the differential equation of a ray in spherical coordinates. The position, direction, and travel time of the seismic wave front at any point along the curved ray path are obtained by numerical integration of the differential equation for an assumed three-dimensional, continuous velocity distribution. The problem of representing a realistic three-dimensional velocity structure in the earth is solved in a way that is especially suitable for use on computers. Some examples for rays traversing an island-arc structure are presented. The implications of this method of tracing rays in a laterally heterogeneous earth are discussed with respect to seismic travel-time studies, interpretation of residuals in terms of tectonic heterogeneities, source bias, and the precise location of earthquakes and nuclear explosions; $dT/d\Delta$ measurements from large seismic arrays and their inversion to obtain details of the velocity structure in the upper mantle are also discussed.

Since the beginning of instrumental seismology and throughout the first half of this century, seismologists have usually treated the seismic velocity structure of the earth's interior as spherically symmetric. It was not until 1933 that Gutenberg suggested that errors due to the earth's ellipticity might be significant for teleseismic travel times, and hence ellipticity should then be taken into account [*Gutenberg and Richter*, 1933]. Jeffreys subsequently derived a method to correct travel times for ellipticity for any given epicenter-station configuration [*Jeffreys*, 1935]. Besides ellipticity, no other lateral variations in the seismic velocities of the upper mantle were emphasized until 10 or 20 years ago, though regional variations in the thickness and structure of the continental and oceanic crust gradually became evident.

Numerous geophysical studies in the last two decades demonstrate a consistent global pattern of strong lateral variations of seismic velocities and other physical properties not only in the earth's crust but also of the upper 700 km of the mantle. These heterogeneities are closely related to major tectonic features such as island arcs, mid-oceanic ridges, rift and fracture zones, and orogenic belts. It is surprising that, despite the accumulating evidence, no suitable method has been available until now for calculating ray paths and travel times of seismic body waves through a laterally heterogeneous earth.

It is the purpose of this study to fill that gap by presenting a basic, computer-oriented method of tracing seismic rays, either for P or S waves, propagating through a laterally heterogeneous spherical earth. This method is especially designed to consider a class of lateral seismic heterogeneities related to sea-floor spreading and global tectonics, e.g., the deep structure beneath mid-oceanic ridges and island arcs, the sources and sinks, respectively, in a system of drifting lithospheric plates.

The plan for this paper is: (1) to describe

[1] Lamont-Doherty Geological Observatory Contribution 1580.

Copyright © 1970 by the American Geophysical Union

the geometric representation of lateral heterogeneities; (2) to derive the differential equations for a ray from Fermat's principle; (3) to present a numerical scheme for the integration; (4) to discuss some of the ray characteristics in a laterally heterogeneous earth; (5) to give an example for applying the ray-tracing method to travel-time studies; and (6) to discuss some of the seismological implications of the new ray-tracing method.

Geometrical Representation of Lateral Heterogeneities

Any point in a spherical earth can be described by means of a spherical coordinate system, r, θ, λ; r is the distance (in kilometers) from the earth's center, θ is the polar distance (in degrees) from the north pole, and λ is the geographical longitude (in degrees), with positive λ east of Greenwich and negative λ west of Greenwich. The limits for the coordinates r, θ, λ are

$$\begin{aligned} 0\text{ km} \leq r &\leq R \\ 0^\circ \leq \theta &\leq 180^\circ \\ -180^\circ \leq \lambda &\leq +180^\circ \end{aligned} \qquad (1)$$

R is the radius of the earth.

Major lateral heterogeneities of the earth are associated with the tectonic structure of island arcs and mid-oceanic ridges. The seismicity and tectonic features of island arcs are described in detail by *Katsumata* [1960], *Sykes* [1966], *Oliver and Isacks* [1967], *Utsu* [1967], and *Mitronovas et al.* [1969] among others. The inclined zone of seismic foci approximately coincides with the descending lithospheric plate that is characterized by low attenuation (high Q) and high seismic velocities. Such slabs of lithosphere extend from the trench down into the mantle beneath the belt of active volcanoes to a maximum depth of about 700 km. In contrast to the descending plate, low seismic mantle velocities and high attenuation (low Q) are observed in a broad zone on the landward side of the volcanic belt.

To map the subsurface boundaries of the different tectonic units, it is convenient to determine contour lines at various depths $h(\theta, \lambda) = \text{constant}$ on the interfaces separating adjacent heterogeneous bodies. As pointed out before, the seismic zone beneath an island arc approximately defines the dipping lithospheric plate. *Sykes* [1966], *Sykes et al.* [1969], and *Katsumata and Sykes* [1969] projected precisely relocated hypocenters on vertical sections perpendicular to that seismic zone in several island arcs in the Pacific. Similar studies were carried out by, among others, *Hamilton and Gale* [1968] for New Zealand and *Katsumata* [1960] and *Utsu* [1967] for Japan. From such sections or from hypocenter maps it is possible to contour the surface of the dipping seismic zone in each active arc. Figure 1 shows as an example a contour map of the seismic zone in the Fiji–Tonga–Kermadec arc. The contours were derived from seismic events reported by the U.S. Coast and Geodetic Survey (CGS) for the period 1961 to 1968. To store information on the depth contours for use in a computer, longitudes λ_{ij} are read for the intersections of each contour h_i with equally spaced colatitudes θ_j. This sampling procedure is suitable only for predominantly N–S striking tectonic features. For an E–W striking feature, a corresponding scheme has to be used; polar distances θ_{ij} are determined for the intersections of contours h_i with equally spaced longitudes λ_j.

Table 1 contains the longitudes λ_{ij} sampled along the contours h_i for the seismic zone in the Fiji–Tonga–Kermadec area shown in Figure 1. This table demonstrates schematically how the information of an arcuate structure is stored in the computer. So far, however, only an arcuate dipping surface has been represented. To provide the dipping plate with some volume, one has to assign horizontal thicknesses a and b, respectively, on each side of the seismic surface, which will be labeled S from now on. This configuration is schematically demonstrated in Figure 2 with a section of an arc. The horizontal distances a and b are measured perpendicular to the strike of each depth contour h_i and for each colatitude interval $[\theta_j, \theta_{j+1}]$. The thickness a is on the concave side of the seismic surface (toward the volcanoes), and b is on the convex side (toward the ocean). The two defined boundaries of the dipping plate are called A and B, respectively; the individual faces comprising A and B are parallel to the corresponding faces of S in each depth interval $[h_i, h_{i+1}]$ and in each polar distance interval $[\theta_j, \theta_{j+1}]$.

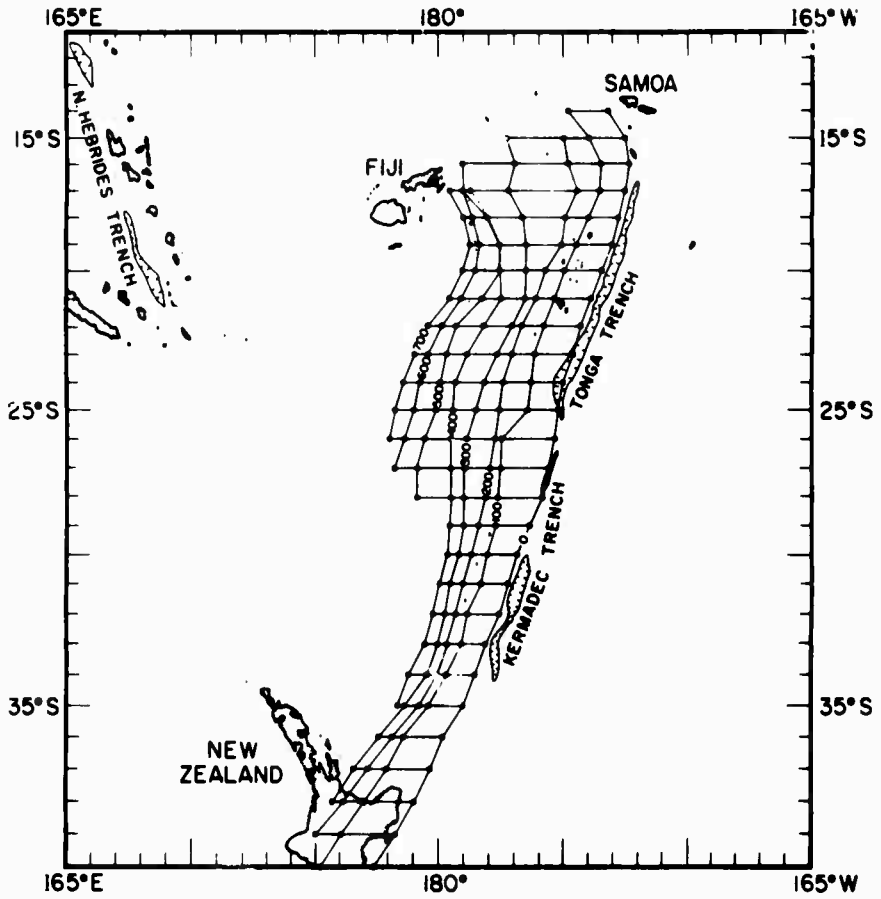

Fig. 1. Representation of the dipping seismic zone in the Tonga–Kermadec island arc by means of depth contours h = constant. The numbers on the contours are depths in kilometers below the earth's surface. Open circles show points of intersection with latitude ϕ = constant; their longitudes λ are compiled in Table 1.

In the unlikely case that the plate thickness or distance between S and A or B is of the same order of magnitude as the radius of curvature of the arc, then A or B, respectively, is no longer a smooth boundary but is an irregular surface composed of facets with small offsets at each sampling value of the polar distance θ_j. These offsets can be kept small, however, if a sufficiently small sampling interval $d\theta$ is used. A certain degree of irregularity in the interfaces A and B can be tolerated because the offsets are smoothed in the specific numerical approach used for describing individual seismic rays. For the dipping plate limited by the surfaces A and B, a seismic velocity is assigned that is higher by a certain percentage δv_{AB} than the velocity at the corresponding depth in the mantle outside the plate. Hence the boundaries A and B represent discontinuities in seismic velocities. This velocity differential is superimposed on a standard velocity distribution for the mantle [e.g., *Jeffreys and Bullen*, 1940, 1948; *Herrin et al.*, 1968], which is a continuous function of depth only.

The existence of a region of low seismic velocities beneath and adjacent to the volcanic belt was discussed by *Mitronovas* [1969], *Utsu* [1967], *Molnar and Oliver* [1969], and *Kanamori* [1970], among others. *Karig* [1970] found indications of young extensional tectonic features to the west of the volcanic belt in the Tonga–Kermadec and Philippine arcs. Thus the zone of low velocity behind island arcs might be related to some kind of local ocean-floor spreading. To account for such a region of lower velocities, another interface C is introduced to form a wedge-shaped body of depth d, and of width c_0 at the earth's surface, as shown in Figure 2. The facets of the interface C also parallel the seismic zone S in the interval-

TABLE 1. Numerical Representation of the Seismic Zone of the Tonga-Kermadec Island Arc

South Latitude, deg	Longitudes, deg							
	h = 700 km	h = 600 km	h = 500 km	h = 400 km	h = 300 km	h = 200 km	h = 100 km	h = 0 km
14	...	...	...	...	...	...	−174.8	−173.2
15	...	...	...	...	−177.3	−175.0	−174.0	−172.5
16	...	...	...	−179.0	−176.9	−174.8	−173.6	−172.4
17	−179.5	−179.0	−178.7	−179.0	−177.2	−174.5	−173.6	−172.5
18	−178.9	−178.6	−178.1	−178.0	−176.7	−174.9	−174.0	−172.8
19	−178.7	−178.3	−177.5	−177.5	−176.5	−175.1	−174.5	−173.1
20	−179.0	−178.5	−177.5	−177.5	−176.5	−175.7	−175.0	−173.5
21	−179.5	−179.1	−178.3	−177.5	−176.5	−176.1	−175.4	−173.9
22	+179.7	−179.8	−179.4	−178.2	−177.0	−176.6	−175.8	−174.3
23	+179.1	+179.7	−179.7	−178.8	−177.7	−177.1	−176.2	−174.6
24	+178.6	+179.3	−179.9	−179.3	−178.2	−177.4	−176.3	−175.0
25	+178.3	+179.1	+179.9	−179.4	−178.5	−177.5	−176.4	−175.2
26	+178.1	+178.7	+179.5	−179.5	−178.8	−177.7	−177.5	−175.3
27	...	+178.4	+179.2	−179.5	−178.9	−177.9	−177.5	−175.6
28	...	...	+179.1	−179.5	−178.9	−178 1	−177.6	−175.8
29	...	...	...	−179.5	−178.9	−178.4	−177.7	−176.3
30	...	...	...	−179.6	−179.2	−178.7	−178.0	−176.8
31	...	...	...	−179.9	−179.5	−179.0	−178.3	−177.2
32	...	...	...	+179.8	−179.7	−179.3	−178.8	−177.6
33	...	...	...	+179.5	+180.0	−179.6	−179.1	−178.1
34	...	...	...	+178.8	+179.6	+180.0	−179.1	−178.5
35	...	...	...	+178.4	+178.7	+179.3	+179.7	−179.0
36	...	...	...	...	+177.6	+178.2	+178.6	−179.8
37	...	...	...	...	+176.6	+177.2	+177.9	+179.7
38	...	...	...	...	+175.6	+176.2	+177.0	+179.1
39	...	...	...	...	...	+175.0	+176.1	+178.3
40	...	...	...	...	...	...	+175.2	+177.4

Longitudes are sampled at the intersections of depth contours h = constant with parallels at latitudes ϕ = constant.

$[\theta_j, \theta_{j+1}]$. The horizontal distance between S and C at any depth $h \leq d$ is defined as

$$c(h) = c_0 - (c_0 - a)h/d \qquad (2)$$

and is measured perpendicular to the local strike of S. According to (2), C approaches A at depth d, indicated by the point D in Figure 2. The wedge-shaped volume is bounded by A, C, and the surface of the earth. The velocity inside this wedge can be chosen to be a certain percentage δv_{AC} lower than the normal mantle velocities for any depth $h \leq d$. To describe the gross seismotectonic features of an island-arc system as presently conceived, it is thus necessary to define only six parameters a, b, c_0, d, δv_{AB}, and δv_{AC}. In addition the coordinates of the depth contours of the seismic zone S must be specified.

Fermat's Principle and Euler's Differential Equations of the Ray

The main purpose of this study is to provide a method of tracing seismic rays through an arbitrary velocity structure. To some extent we follow the approach of *Sattlegger* [1964], who treated a similar problem in a Cartesian space for seismic reflection surveys. Instead of using the velocity function $v(r, \theta, \lambda)$ to describe the velocity structure of the earth, we use here the more suitable quantity slowness $u(r, \theta, \lambda)$, the reciprocal of the velocity. We assume that the scalar u is a continuous function throughout the earth. Hence, any first-order discontinuity in slowness u is replaced by a zone of gradual change in u. To allow application of ordinary ray theory, the magnitude of the gradient of u must be kept reasonably small. Thus, for a given contrast in slowness u, the

zone of gradual change in u has to be wide enough to keep the gradient of u small.

According to Fermat's principle a seismic ray will choose the specific path S that takes the least travel time T to propagate from a point A to a point B:

$$T = \int_A^B u(l_i l_i)^{1/2}\, ds = \text{Extremum} \qquad (3)$$

where l_i is the tangent vector at any point along the ray with its components

$$l_i = (r', r\theta', r \sin \theta \lambda') \qquad (4)$$

The quantities r', θ', λ' are the derivatives of the coordinates along the ray increment ds and represent the components of direction of the ray. Multiplied by their respective metric factors l, r, and $r \sin \theta$ for a spherical coordinate system, they form the components of a unit tangent vector where

$$(l_i l_i)^{1/2} = 1 \qquad (5)$$

and the summation convention applies.

The problem stated in equation 3 is common in the calculus of variation. It can be solved by finding solutions to the corresponding set of Euler's differential equations. They are obtained by defining the integrand $u(l_i l_i)^{1/2}$ of equation 3 as the Euler function $F(g_i, g_i')$, where g_i stands for the generalized coordinates and g_i' for their derivatives; the differential equations take the following form:

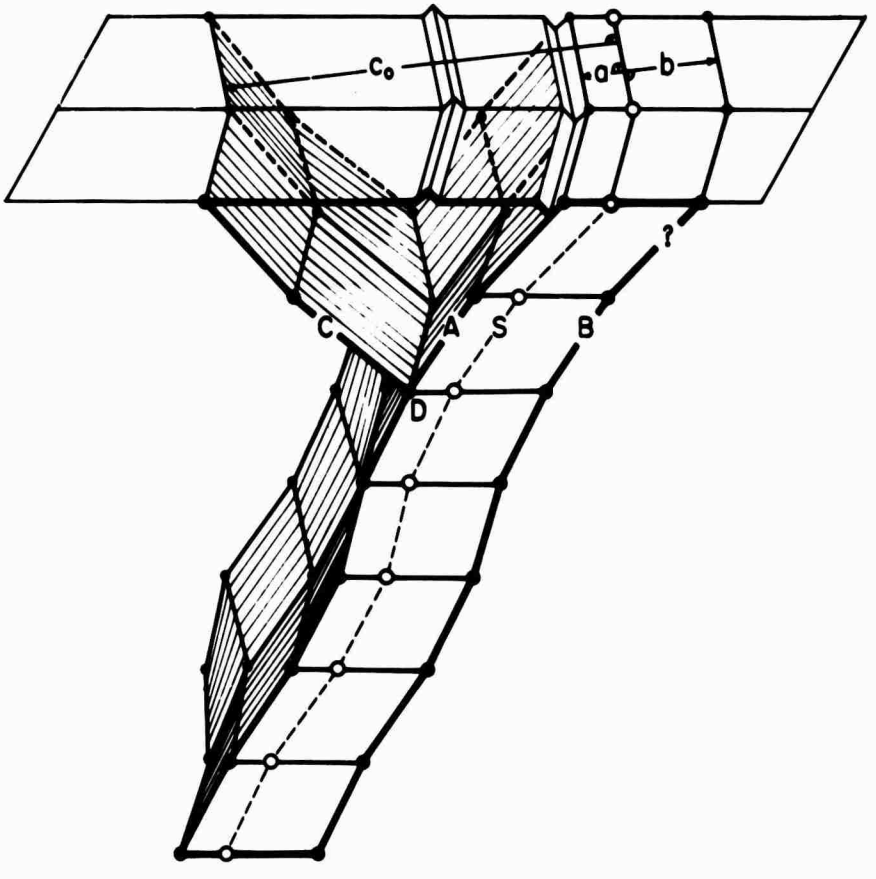

Fig. 2. Section of an island arc structure showing schematically the geometry of the model used for representing lateral heterogeneities related to the deep seismic zone. S = seismic zone; A = upper boundary of the descending plate of lithosphere; B = lower interface of the descending plate; C = boundary on the continental side of the wedge-shaped low-velocity body near the volcanic belt; D = deepest point of the low-velocity wedge at depth d. Open circles on S represent sampled points shown also in Figure 1 and Table 1. For details of measuring the horizontal distances a, b, and c, see text. The question mark in the upper part of B indicates that the model does not represent here the actual boundary of the lithospheric plate very well.

$$E_i = \frac{d}{ds}\left(\frac{\partial F}{\partial g_i'}\right) - \frac{\partial F}{\partial g_i} = 0 \qquad (6)$$

From (4), (5), and (6) we obtain

$$\frac{d}{ds}(ur') - \frac{\partial u}{\partial r} - ur(\theta'^2 + \lambda'^2 \sin^2\theta) = 0$$

$$\frac{d}{ds}(ur^2\theta') - \frac{\partial u}{\partial \theta} - \tfrac{1}{2}ur^2\lambda'^2 \sin 2\theta = 0 \qquad (7)$$

$$\frac{d}{ds}(ur^2\lambda' \sin^2\theta) - \frac{\partial u}{\partial \lambda} = 0$$

The remaining differentiation of the first term and rearranging of all resulting terms yields the following expressions for the second derivatives r'', θ'', λ'':

$$r'' = (1/u)\left(\frac{\partial u}{\partial r} - u'r'\right) + r(\theta'^2 + \lambda'^2 \sin^2\theta)$$

$$\theta'' = \frac{1}{ur^2}\frac{\partial u}{\partial \theta} + \tfrac{1}{2}\lambda'^2 \sin 2\theta - \theta'\left(\frac{u'}{u} + 2\frac{r'}{r}\right) \qquad (8)$$

$$\lambda'' = \frac{1}{ur^2 \sin^2\theta}\frac{\partial u}{\partial \lambda} - \lambda'\left(\frac{u'}{u} + 2\frac{r'}{r} + 2\frac{\theta'}{\tan\theta}\right)$$

where

$$u' = \frac{\partial u}{\partial s} = \frac{\partial u}{\partial r}r' + \frac{1}{r}\frac{\partial u}{\partial \theta}\theta' + \frac{1}{r\sin\theta}\frac{\partial u}{\partial \lambda}\lambda' \qquad (9)$$

The equations 8 are the differential equations of the seismic ray in terms of components of ray curvature r'', θ'', λ'' anywhere in a spherical earth that has a continuous slowness distribution $u(r, \theta, \lambda)$. The ray curvature depends, first, on the components of the gradient of slowness $(\partial u\ \partial r)$, $(\partial u\ \partial \theta)$, $(\partial u\ \partial \lambda)$ and, second, on the direction of the ray with respect to the direction of the gradient of slowness. The second relation is concealed in equation 9 for $u' = \partial u\ \partial s$. It represents the projection (Scalar product) of the gradient of slowness on the tangent vector of the ray.

Expansion of Ray Coordinates into a Taylor Series

Any attempt to find the actual ray path by analytical integration of (8) for a realistic slowness function $u(r, \theta, \lambda)$ is likely to fail. Instead of an analytical integration of (8), we try stepwise numerical integration by a finite-series scheme, a method similar to that used by *Sattlegger* [1964, 1969].

The behavior of a seismic ray s in the vicinity of a point $P_0(r_0, \theta_0, \lambda_0)$ on the ray can be described by expanding the ray coordinates r, θ, λ and travel time t in a Taylor series:

$$\begin{aligned} r &= r_0 + r_0'\,ds + \tfrac{1}{2}r_0''\,ds^2 + \cdots \\ \theta &= \theta_0 + \theta_0'\,ds + \tfrac{1}{2}\theta_0''\,ds^2 + \cdots \\ \lambda &= \lambda_0 + \lambda_0'\,ds + \tfrac{1}{2}\lambda_0''\,ds^2 + \cdots \\ t &= t_0 + u_0\,ds + \tfrac{1}{2}u_0'\,ds^2 + \cdots \end{aligned} \qquad (10)$$

All values forming the zero-, first-, and second-order terms on the right-hand side of (10) are either known or can be calculated from (8) and (9) if the slowness $u(r, \theta, \lambda)$ is given; r_0, θ_0, λ_0 and t_0 represent the initial position and the origin time of the ray at the point P_0'; r_0', θ_0', λ_0' represent the initial direction of the ray that can be prescribed. Finally, r_0'', θ_0'', λ_0'' are the elements of ray curvature and can be calculated from (8) and (9). If the spatial gradient of slowness u varies slowly, the higher order terms do not contribute significantly to the sum in (10). The error in neglecting these terms can be kept arbitrarily small by proceeding only in small increments ds. After the first step ds, the ray has propagated from $P_0(r_0, \theta_0, \lambda_0, t_0)$ to $P(r, \theta, \lambda, t)$. The new direction of the ray point $P(r, \theta, \lambda, t)$ can be obtained by differentiating (10):

$$\begin{aligned} r' &= r_0' + r_0''\,ds + \cdots \\ \theta' &= \theta_0' + \theta_0''\,ds + \cdots \\ \lambda' &= \lambda_0' + \lambda_0''\,ds + \cdots \end{aligned} \qquad (11)$$

Only the first two terms in (11) must be considered to keep the accuracy of the computation consistent with that in equation 10. Terms of higher order can be neglected again for the proper choice of ds.

Using r, θ, λ from (10), r', θ', λ' from (11), and r'', θ'', λ'' from (8), we may trace the ray

from point to point in steps ds until the ray emerges somewhere at the earth's free surface.

Numerical Scheme

To let the ray propagate point to point, say from P_k to P_{k+1}, one has to determine the components of curvature of the ray r'', θ'', λ'', or, according to equation 8, to find the gradient of slowness ($\partial u/\partial r$, $\partial u/\partial\theta$, $\partial u/\partial\lambda$) in the vicinity of P_k. It is obvious that the gradient of u at an intermediate point $P_{k+1/2}$ is more representative of the curvature for the ray path between P_k and P_{k+1} than the gradient at the end point P_k. Thus the accuracy of the numerical integration could be improved. Unfortunately, it is not possible to determine the location of the point $P_{k+1/2}$ and consequently the gradient of this point, because the curvature for the ray between P_k and P_{k+1} is not known in advance. To find an approximate location of $P_{k+1/2}$, however, we may use the curvature of the previous ray element determined at $P_{k-1/2}$ and extrapolate the ray path beyond P_k by half an increment $ds/2$. Accordingly, the following numerical scheme is used for the ray-tracing procedure:

1. Find the auxiliary point $P_{k+1/2}$ by extrapolating the previous ray element beyond P_k by an increment $ds/2$:

$$\begin{aligned} r_{k+1/2} &= r_k + \tfrac{1}{2}r_k'\,ds + \tfrac{1}{8}r_{k-1/2}''\,ds^2 \\ \theta_{k+1/2} &= \theta_k + \tfrac{1}{2}\theta_k'\,ds + \tfrac{1}{8}\theta_{k-1/2}''\,ds^2 \\ \lambda_{k+1/2} &= \lambda_k + \tfrac{1}{2}\lambda_k'\,ds + \tfrac{1}{8}\lambda_{k-1/2}''\,ds^2 \end{aligned} \tag{12}$$

2. Determine the slowness of u and its gradient ($\partial u\ \partial r$, $\partial u\ \partial\theta$, $\partial u\ \partial\lambda$) at the auxiliary point $P_{k+1/2}$ and use these data in equations 8 and 9 to calculate the curvature components.

3. Let the ray propagate from P_k to P_{k+1} with a step ds according to

$$\begin{aligned} r_{k+1} &= r_k + r_k'\,ds + \tfrac{1}{2}r_{k+1/2}''\,ds^2 \\ \theta_{k+1} &= \theta_k + \theta_k'\,ds + \tfrac{1}{2}\theta_{k+1/2}''\,ds^2 \\ \lambda_{k+1} &= \lambda_k + \lambda_k'\,ds + \tfrac{1}{2}\lambda_{k+1/2}''\,ds^2 \\ t_{k+1} &= t_k + u_{k+1/2}\,ds \end{aligned} \tag{13}$$

4. The direction of the ray at the new point P_{k+1} is given by

$$\begin{aligned} r_{k+1}' &= r_k' + r_{k+1/2}''\,ds \\ \theta_{k+1}' &= \theta_k' + \theta_{k+1/2}''\,ds \\ \lambda_{k+1}' &= \lambda_k' + \lambda_{k+1/2}''\,ds \end{aligned} \tag{14}$$

5. Repeat steps 1 through 4 with all subscripts increased by one integer unit, and continue until the ray reaches the earth's free surface.

The slowness and its gradient components are determined for step 2 of that scheme by one of the following two methods, depending on whether the ray penetrates a zone with or without lateral heterogeneities present.

(a) *In the presence of lateral heterogeneities*: Assume a cube centered around the auxiliary point $P_{k+1/2}$ with an edge length $2w$. Its eight corner points are labeled Q_{lmn} where the subscript l, m, or n may take either the value 1 or 2, depending on whether its corresponding coordinate r, θ, and λ of the point Q_{lmn} is smaller or larger than that of the auxiliary point $P_{k+1/2}$.

Thus these eight points Q_{lmn} are located at

$$\begin{aligned} Q_{111} &= (r - w,\ \theta - w/r,\ \lambda - w/r\sin\theta) \\ Q_{211} &= (r + w,\ \theta - w/r,\ \lambda - w/r\sin\theta) \\ &\vdots \\ Q_{222} &= (r + w,\ \theta + w/r,\ \lambda + w/r\sin\theta) \end{aligned} \tag{15}$$

The slowness at each point Q_{lmn} is called u_{lmn}. From these eight values of slowness we derive the arithmetic mean and assign it to the slowness at point $P_{k+1/2}$.

$$\begin{aligned} u_{k+1/2} = (&u_{111} + u_{112} + u_{121} + u_{122} \\ &+ u_{211} + u_{212} + u_{221} + u_{222})/8 \end{aligned} \tag{16}$$

By calculating the average of the slowness of 4 points at the higher value of one specific coordinate and subtracting it from the average slowness of 4 points at the lower value of that coordinate, one can obtain the components of the slowness gradient for this coordinate:

$$\begin{aligned} \partial u/\partial r &= [(u_{222} + u_{221} + u_{212} + u_{211}) \\ &\quad - (u_{111} + u_{121} + u_{112} + u_{122})]/8w \\ \partial u\ \partial\theta &= [(u_{121} + u_{122} + u_{221} + u_{222}) \\ &\quad - (u_{111} + u_{112} + u_{211} + u_{212})]/(8w/r) \\ \partial u\ \partial\lambda &= [(u_{112} + u_{122} + u_{212} + u_{222}) \\ &\quad - (u_{111} + u_{121} + u_{211} + u_{221})]/(8w/r\sin\theta) \end{aligned} \tag{17}$$

It is now easy to understand how the sharp discontinuities in slowness u associated with the tectonic features described in a previous section are smoothed out to gradient zones with a finite thickness. That thickness varies between $2w$ and $2w(3)^{1/2}$, depending on the relative local orientation of the auxiliary cube Q_{lmn} that is carried along with the ray as it propagates. The auxiliary cube detects the orientation of the interface by averaging over the gradients determined at successive points $P_{k-1/2}$, $P_{k+1/2}$, $P_{k+3/2}$, . . . ; during each step the gradient depends on which of the eight points Q_{lmn} are found to be inside a lateral heterogeneity or outside in the regular mantle. To guarantee a satisfactory averaging of gradients while passing through a transition zone, the ray must propagate for many steps inside that gradient zone. This can be assured if the step size ds is kept small compared to the length $2w$ of the gradient cube. Consequently, a provision has been made in the computer program to detect whether any of the components of the gradient exceeds a limit by using the following criterion:

$$\left|\frac{\partial u}{\partial r}\right| + \left|\frac{1}{r}\frac{\partial u}{\partial \theta}\right| + \left|\frac{1}{r \sin \theta}\frac{\partial u}{\partial \lambda}\right| \leq G \qquad (18)$$

where G is of the order of 0.1×10^{-4} sec/km^2.

If condition 18 holds, no unusual boundary is present and ds is generally chosen to be about 1 to 2 km; the cube length $2w$ is kept of the order of 2 to 4 km. If, however, condition 18 does not hold because a strong gradient zone is being approached, then ds will be lowered to 0.1 or 0.2 km while keeping $2w$ constant at 2 to 4 km. This allows for at least 20 steps for ray propagation through a gradient zone replacing the sharp discontinuity.

(*b*) *In the absence of lateral heterogeneities*: In the case where there are no lateral heterogeneities present, the calculation of $u_{k+1/2}$ and of its gradient can be reduced considerably by using the slowness u_2 and u_1 of only two points just above and below the auxiliary point $P_{k+1/2}$.

$$\begin{aligned} Q_2 &= (r_{k+1/2} + w,\ \theta_{k+1/2},\ \lambda_{k+1/2}) \\ Q_1 &= (r_{k+1/2} - w,\ \theta_{k+1/2},\ \lambda_{k+1/2}) \end{aligned} \qquad (19)$$

The slowness u assigned to the vicinity of the auxiliary point $P_{k+1/2}$ is

$$u_{k+1/2} = (u_2 + u_1)/2 \qquad (20)$$

and the components of the gradient of u are

$$\begin{aligned} \partial u/\partial r &= (u_2 - u_1)/2w \\ \partial u/\partial \theta &= \partial u/\partial \lambda = 0 \end{aligned} \qquad (21)$$

It is important to note that the method used here breaks down in a narrow cylinder extending from the south to the north pole along the rotational axis of the spherical coordinate system because of singularities in the denominator of some terms of (8) and (9) at $r = 0$ and $\theta = 0°$ and $\theta = 180°$. Rays which penetrate into that cylinder with a critical radius of about 10 km must be omitted.

Additional Information from the Ray Trace

The ray-tracing procedure as described above provides information on the ray r, θ, λ at discrete points P_k, the direction r', θ', λ' at these points, the travel time t, and the cumulative paths along the ray. From some of these data and the stored data on slowness $u(r, \theta, \lambda)$, additional information can be obtained to describe some ray characteristics that are commonly used in seismology, e.g., $dt/d\Delta$ along the ray, azimuth α (measured clockwise from north in a horizontal plane), and angle of emergence i.

Relations between r', θ', λ' and the strike α and angle of emergence i (as measured from the downward vertical) can be found from simple geometry:

$$\begin{aligned} r' &= -\cos i \\ \theta' &= -\sin i \cos \alpha / r \\ \lambda' &= \sin i \sin \alpha / (r \sin \theta) \end{aligned} \qquad (22)$$

The corresponding inverse relations are

$$\begin{aligned} \alpha &= \tan^{-1}(\lambda' \sin \theta / -\theta') \\ i &= \tan^{-1}[r(\lambda'^2 \sin^2 \theta + \theta'^2)^{1/2} / -r'] \end{aligned} \qquad (23)$$

Note that, while α may lie in any of the 4 quadrants, i can lie only in the first and second quadrant.

An important quantity in classical ray theory with spherically symmetric velocity structure $v(r)$ is the ray parameter $p = dt/d\Delta$, which is a constant value for any individual ray along its entire path. The ray parameter p or $dt/d\Delta$ is the inverse apparent velocity, or the slowness

of the trace of the ray projected to the earth's surface at $r = R$ and is defined as

$$dt/d\Delta = 111.195u(r, \theta, \lambda) \sin i\, r/R \qquad (24)$$

with $dt/d\Delta$ measured in seconds per degree, u in seconds per kilometer, and r and R in kilometers. It is a characteristic feature that this 'ray parameter' is no longer a constant value along each ray if the velocity is a function of all 3 coordinates, $v = v(r, \theta, \lambda)$. Thus monitoring of $dt/d\Delta$ along the ray during the computation can be used to indicate whether the ray propagates through a lateral heterogeneity or not, depending on whether $dt/d\Delta$ varies or remains constant. The consequences of a variable $dt/d\Delta$ for any ray passing through a lateral heterogeneity are extremely important for any study using $dt/d\Delta$ data measured at large seismic arrays. The common but false assumption that v varies only with depth can yield unrealistic or at least inaccurate results for the velocity structure. This important subject is further investigated in a separate paper.

Before applying the ray-tracing method to interpret observed patterns of travel-time residuals, an important characteristic of *computed* residuals must be recognized. Computed residuals depend essentially on the geometry and magnitude of lateral heterogeneities and very little or not at all on the specific earth model used for reference. Hence it is irrelevant to the computed residuals if a velocity distribution of Jeffreys and Bullen, Herrin and his associates, or any other reasonable earth model is used as standard for the laterally homogeneous parts of the earth's mantle. The standard model chosen is not essential because the travel times for the standard earth with superimposed heterogeneities are compared to travel times of the standard earth without heterogeneities. Thus the travel times for the standard earth cancel when the residuals are computed.

The situation is different for *observed* residuals. Observed residuals depend on the standard model used because there is usually some unknown difference between the assumed standard earth and the real average earth representing the tectonically nonactive parts of the mantle. Thus, when observed residuals are obtained, the travel times for the actual (but normal) parts of the earth do not cancel with the travel times for the adopted standard model. Hence the observed residuals are not purely generated by lateral heterogeneities but are somewhat falsified by a systematic difference between the actual and the adopted standard earth.

Only the so-called 'relative residuals' as employed by *Mitronovas* [1969] in his study of the Fiji-Tonga area do not depend on any assumed velocity standard. We shall refer to these data in the following section.

Application to Tonga–Kermadec Arc

To illustrate the application of the ray-tracing method to seismic travel-time studies, an example is presented for a geographic region where the existence of a lateral heterogeneity is well established. The Tonga–Kermadec arc is one of the most thoroughly studied of the active island arcs. The spatial distribution of the seismicity is described by *Sykes* [1966] and *Sykes et al.* [1969]; the seismic focal mechanisms and their tectonic implications for that region are discussed by *Isacks et al.* [1969]; wave propagation, absorption phenomena, and travel-time anomalies were investigated by *Oliver and Isacks* [1967], *Mitronovas* [1969], and *Mitronovas et al.* [1969].

To illustrate the effect of lateral seismic heterogeneities of the Tonga–Kermadec arc on travel times, computed arrival times of traced rays are compared to P travel times observed at local stations from deep sources. P arrivals at teleseismic distances from shallow events in the Fiji–Tonga region are also considered. All the observational data used for comparison are taken from the study of *Mitronovas* [1969]. The velocity model adopted for the calculation is shown in the lower part of Figure 3. It illustrates a vertical section through the island arc with the plate dipping into the mantle. The section cuts through an assumed hypocenter located inside the plate at $\phi = 20°S$ and $\lambda = 179°W$ at a depth of 600 km. The profile strikes N70°W perpendicular to the Tonga trench. The shortest distance to the trench is about 4.8° to the ESE from the assumed epicenter. The geometry of the descending slab was simplified compared to that outlined in Figure 1 to make it compatible with the slab geometry used by *Mitronovas* [1969]. Undulations of the seismic zone below 100 km were removed, yielding a planar slab dipping at

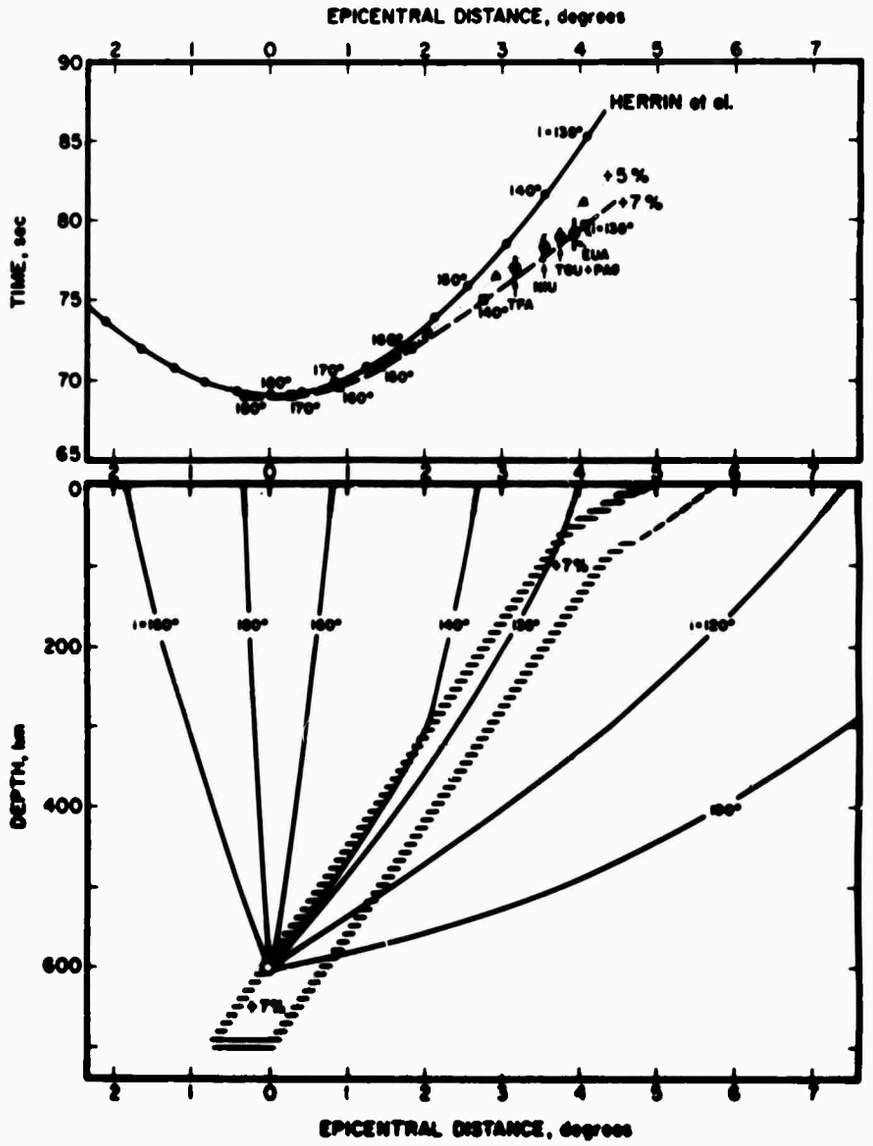

Fig. 3. (*Bottom*) Vertical section through the Tonga arc perpendicular to the strike of the arc. The geometry of the lithospheric plate below $h = 100$ km is simplified to a planar slab. Numbers on the traced rays (solid lines) are take-off angles i for a source at a depth at 600 km. (*Top*) P travel times versus epicentral distance for various cases. The solid line and open circles indicate a normal mantle with a velocity distribution according to *Herrin et al* [1968] without a dipping lithosphere; the dotted line and triangles show a slab with a velocity 5% higher than that of the regular mantle; the dashed line and squares indicate a 7% higher P velocity. Numbers along the curves indicate the take-off angle i for several rays at the source. Solid circles with error bars and station labels are observed travel times from *Matumoto* [1969].

about 55° for depths of 100 to 700 km. In the upper 100 km the dip of the plate decreases to about 30° near the trench. The horizontal dimension of the plate was chosen to be 100 km. The P-velocity distribution of *Herrin et al* [1968] was adopted for the mantle outside the slab, while a 7% higher P velocity was assumed inside the slab in one case and a 5% higher velocity in another case. In this model no low-velocity zone was assumed beneath and adjacent to the volcanic ridge. The upper part of Figure 3 shows the corresponding travel-time curves calculated with the ray-tracing program. The solid line through open

circles is the regular Herrin travel time with no dipping plate present. The dotted line through open triangles corresponds to *P* arrivals with a 5% higher velocity inside the plate and the dashed line through open squares to *P* arrivals with a 7% higher velocity. The computed travel times show clearly that the *P* waves arrive increasingly earlier (compared to the Herrin travel times) the further the rays propagate through the fast, dipping lithospheric plate. Thus rays emerging at larger distances close to the trench are associated with larger negative residuals (up to −6 sec) than those farther away from the trench and closer to the epicenter.

Superimposed on the calculated travel times are observed travel times from 5 stations in the Tonga island arc. To obtain the 'observed' travel times for those stations, 'relative residuals' determined by *Mitronovas* [1969] were subtracted from the Herrin travel times at corresponding epicentral distances. Mitronovas attempted, first, to eliminate the source bias for all events studied, using only those near and distant stations for the relocation for which the seismic rays bypass major heterogeneities in the upper 700 km of the mantle in the Fiji–Tonga region. Second, he obtained 'relative residuals' for local stations in the Fiji–Tonga region. The relative residuals result from a comparison of arrival times at similar epicentral distances in the Tonga and in the Fiji Islands for rays that pass through or bypass, respectively, the dipping plate. These relative residuals for the local stations are to a first approximation independent of the standard travel times used [e.g., *Jeffreys and Bullen*, 1940, 1958; *Herrin et al.*, 1968] and hence are, to a first order, independent of the exact knowledge of the exact origin time of the earthquake. The residuals used in Figure 3 to obtain the 'observed travel time' are the average values obtained by Mitronovas from all available *P* data at the 5 local stations for 38 carefully relocated earthquakes with an average focal depth of about 600 km.

The comparison of observed and calculated *P* travel times shows that the velocity inside the slab is on the average about 6% higher than the mantle velocities outside the plate. Note that this result is, to a first order, independent of the use of a specific standard model for this case Herrin et al.). There is some indication that this velocity contrast increases from about 5% to about 7% as the emerging rays approach the trench. If this trend is confirmed in future studies, three different explanations should be considered. First, the change in velocity contrast is real and such that it decreases with depth inside the plate because of a gradual heating of the cooler plate as it moves downward into the warmer mantle; hence rays penetrating through only the lower part of the plate are slower compared with those penetrating through the upper part with the higher velocity contrast. Second, rays emerging at smaller epicentral distances may propagate a longer distance through a body of lower velocities located near and beneath the volcanic belt, as indicated in Figure 2. Or third, the geometry is more complex. A low-velocity region was not taken into account for the model calculations shown in Figure 3. If the low-velocity region exists, it will increase the estimate for the average velocity contrast of the slab to a higher value of about 7%.

The method of relative residuals is especially suitable for deep events if local stations are available. As shown by *Mitronovas* [1969], the method of relative residuals is not applicable for shallow sources (occurring in the upper part of the plate) with stations at teleseismic distances. Thus residuals at teleseismic distances for shallow earthquakes occurring in the upper part of the plate are dependent on the earth model used for reference. Figure 4 illustrates a typical case showing the geometry of the plate, the source location relative to the plate, and two selected rays traced through the model. Many rays striking only perpendicular to the arc were traced to teleseismic distances and their *P* residuals were calculated by using a Herrin model for the mantle outside the slab and a 7% higher velocity inside the slab. The calculated residuals obtained from ray tracing are plotted in Figure 3 (solid triangles) as a function of epicentral distance. Note again that these *computed* residuals are not affected by the use of Herrin's model. For comparison, the observed residuals of an earthquake near the Tonga Islands reported by *Mitronovas* [1969] are plotted (solid line through open circles). The location of this earthquake with respect to the slab is very similar to that shown in the

model of Figure 4. Thus the two sets of residuals, the calculated and the observed one, can be properly used for comparison. The characteristic parameters of this earthquake are: August 12, 1967, 09h 39m 44.1s, h = 134 km, ϕ = 24.86°S, λ = 177.01°W, m_b = 5.8. The location and origin time were derived by Mitronovas by using data from the local stations only. The residuals were obtained only for rays traversing through the plate in a WNW direction to teleseismic distances. Jeffreys-Bullen (J-B) travel times were used for reference. These J-B residuals were averaged in 10° intervals of epicentral distance. The observed J-B and the calculated residuals shown in Figure 5 have in common that they increase with epicentral distance as the rays propagate along an increasingly longer path inside the slab. Rays that travel the longest possible distance inside the slab emerge at epicentral distances approximately between 50° and 60° and show, as expected, the largest negative residuals. Beyond 60°, the residuals decrease as the rays leave the slab on its lower boundary. It is evident from Figure 5 that the calculated residuals do not decrease rapidly enough in that distance range. This is because the assumed horizontal dimension (200 km) for that model is too large. Reducing the thickness of the plate (to about 100 km as in the previous model) would result in a curve for the calculated residuals that has approximately the same shape as the curve for the observed residuals. Part of the large negative residuals at epicenter distances near 60° could be interpreted alternatively by the relatively large J-B travel times (approximately 2 sec longer than, e.g., Herrin travel times). In our opinion this is, however, more likely an indication that the travel times of Herrin et al. are somewhat too short in this distance range, since they do not yield the large negative residuals expected from the study of deep events in that region. It is not our intention to determine in this paper the shape and size of the dipping slab in the Tonga region by fitting the model so that observed and calculated residuals match in an optimum sense. However, it is clear that by systematic variation of the six model parameters and, if necessary, of the shape of the seismic zone one can

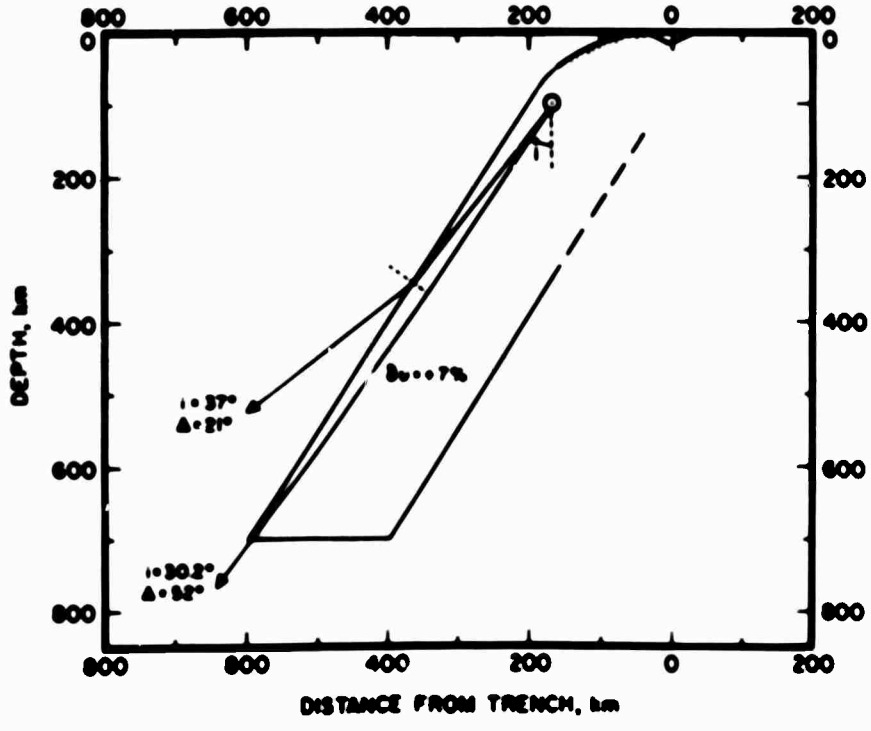

Fig. 4. A model of the slab with a source at depth h = 100 km. This model is used for tracing rays to, and calculating P residuals at, teleseismic distances. Parts of two ray traces with lateral refractions are shown. The calculated P residuals for that model are plotted in Figure 5.

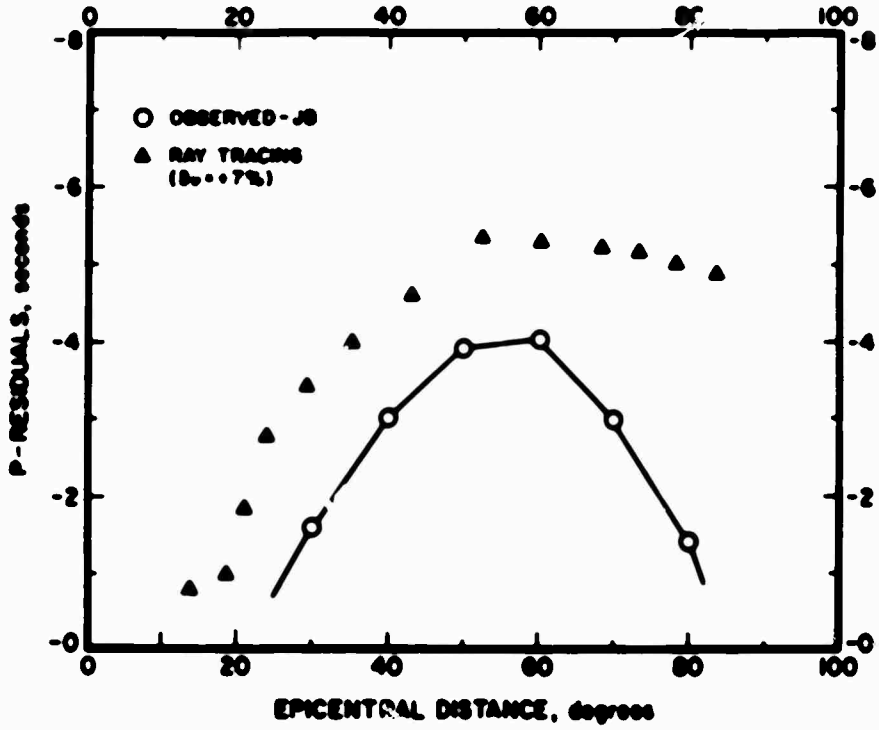

Fig. 5 Comparison of observed P residuals (*Matumoto*, 1960) and theoretical residuals calculated by ray tracing for the model shown in Figure 4. For details see text.

find a combination of parameters that will yield a minimum for the standard deviation between observed and calculated residuals. This method of trial and error may, but does not necessarily, converge toward the actual velocity structure, partially because of the restrictions inherent in the model. Lateral heterogeneities near the receiver or anywhere along the rest of the ray path, and possible differences between the adopted standard model and the actual earth, complicate the problem and introduce nonuniqueness. Further investigations are necessary to consider more rigorous inversion techniques, e.g., those developed by *Backus and Gilbert* [1967, 1968].

There is a DC shift of about 1.5 sec between the observed and the calculated residuals in Figure 5. This offset is primarily due to the uncertainty in the origin time of the earthquake and depends on the specific use of the J-B tables as the travel-time standard for relocation of the event and determination of station residuals. More reliable information can be extracted from residuals of large nuclear explosions for which the origin time and location are known very accurately. The P residuals of the nuclear underground explosion Longshot will be used in a later paper to investigate lateral heterogeneities associated with the Aleutian island arc.

Some Seismological Implications

A basic numerical scheme is presented in this paper for tracing seismic rays through a laterally heterogeneous earth. With this new method it is possible for the first time to calculate on a worldwide scale accurate theoretical residuals of either P or S travel times caused by a global pattern of lateral heterogeneities in the crust and upper mantle. The geometric shape of the tectonic units and heterogeneous bodies can be derived for a first trial model from various sources of information, e.g., from seismicity, the geographic distribution of deep-sea trenches, active volcanoes, mid-oceanic ridges, and other gross tectonic and morphological features. By systematic comparison of theoretical residuals and observed residuals from nuclear explosions as well as earthquakes in various tectonically active regions around the world, the parameters describing the shape and the seismic velocities of the heterogeneities have to be gradually

varied so that the calculated residuals converge toward the observed residuals. First results suggest that this method is a very suitable tool to test some details and consequences of the ideas of plate tectonics.

The information on the lateral variation of seismic velocities can be combined with laboratory results on the dependence of seismic velocities on temperature and pressure in rocks and minerals that are thought to occur in the upper mantle. From the seismic velocities it is then possible to derive information on the temperature regime of descending lithospheric plates in island arcs or of zones of upwelling mantle material beneath mid-oceanic ridges. The 6 to 7% higher P velocity for the descending plate in the Fiji-Tonga-Kermadec region suggests that the sinking lithosphere at a depth of a few hundred kilometers may be several hundred degrees colder than the surrounding mantle [*McKenzie*, 1970; *Mitronovas*, 1969].

Another interesting feature that now can be studied more quantitatively rather than qualitatively is the relation between attenuation of seismic energy, especially of S waves, and seismic velocities and temperature in tectonically active regions of the upper mantle. Favorable places for that kind of study are the Fiji-Tonga-Kermadec arc, New Zealand, Japan, the Aleutian Islands, Hawaii, and Iceland. These sites have in common the advantage that local seismic stations are installed close to strong lateral heterogeneities and that the regional seismic activity is either high or at least moderate.

Ray tracing in a laterally heterogeneous earth will definitely help to improve considerably the accuracy in relocating earthquakes and underground nuclear explosions. For improving the location, the hypocenter and origin time obtained from a routine location procedure can be assumed initially. From the trial location of the source, seismic rays are traced through a laterally heterogeneous earth model to determine the global pattern of theoretical travel-time residuals for the event. The calculated residuals are then used to correct the observed arrival times for lateral effects. Subsequently a conventional relocation is carried out again, but now with the corrected arrival times. This procedure may be used iteratively.

Since this method of tracing seismic rays also provides information on $dt/d\Delta$ along the ray, it can be used to reinterpret $dt/d\Delta$ measurements at large seismic arrays. Consideration of the lateral inhomogeneities, not only directly beneath or near the array but also near the source and along the rest of the ray path, will change somewhat the interpretation of these data with respect to the velocity structure in the upper mantle. Many of the anomalies in $dt/d\Delta$ may be related to inhomogeneities in island arcs and ridges rather than to anomalies in the lower mantle. Array techniques for locating seismic events will also be affected by applying results obtained from three-dimensional ray tracing.

In conclusion, it is evident that the possibility of considering tectonically realistic models of lateral heterogeneities and of tracing seismic rays through laterally variable earth models opens a new dimension in nearly all fields related to seismic travel-time studies. Much of the scatter in travel-time data that until now appeared to be of random nature may turn out to be caused by lateral, deterministic features that are related to global tectonic processes. A thorough study of these travel-time perturbations will yield new insight into the structure and dynamics of the earth's interior. In a forthcoming paper, the ray-tracing method will be applied to some selected problems with special emphasis on the interpretation of the P residuals from the Longshot underground nuclear explosion.

Acknowledgments. I am grateful to W. Mitronovas for furnishing his excellent travel-time data for the Fiji-Tonga region prior to publication and for many discussions with him, as well as to R. Locke and M. Barazangi for their suggestions. I thank J. Oliver for drawing my attention to the problem of three-dimensional ray tracing. L. Sykes, R. Page, and L. R. Sykes for critically reading the manuscript, and K. McCamy for discussions of some computational aspects.

Computing facilities were generously provided by the NASA Goddard Space Flight Center Institute for Space Studies, New York. This research was supported by the Advanced Research Projects Agency of the Department of Defense and was monitored by the Air Force Cambridge Research Laboratories under contract F19628-68-C-0331.

References

Backus, G., and J. Gilbert, Numerical applications of a formalism for geophysical inverse problems, *Geophys. J. 13*, 247, 1967.

Backus, G., and J. Gilbert, The resolving power

of gross earth data, *Geophys. J.*, *16*, 169, 1968.
Gutenberg, B., and C. F. Richter, Advantages of using geocentric latitude in calculating distances, *Beitr. Geophys.*, *37*, 390, 1933.
Hamilton, R. M., and A. W. Gale, Seismicity and structure of North Island, New Zealand, *J. Geophys. Res.*, *73*, 3859, 1968.
Herrin, E., E. P. Arnold, B. A. Bolt, G. E. Clawson, E. R. Engdahl, H. W. Freedman, D. W. Gordon, A. L. Hales, J. L. Lobdell, O. Nuttli, C. Romney, J. Taggart, and W. Tucker, 1968 Seismological tables for *P* phases, *Bull. Seismol. Soc. Amer.*, *58*, 1193–1352, 1968.
Isacks, B., L. R. Sykes, and J. Oliver, Focal mechanisms of deep and shallow earthquakes in the Tonga-Kermadec region and the tectonics of island arcs, *Bull. Geol. Soc. Amer.*, *80*, 1443, 1969.
Jeffreys, H., On the ellipticity correction in seismology, *Mon. Not. Roy. Astron. Soc., Geophys. Suppl.*, *3*, 271, 1935.
Jeffreys, H., and K. E. Bullen, *Seismological Tables*, 50 pp., British Association for the Advancement of Science, Gray-Milne Trust, London, 1940.
Jeffreys, H., and K. E. Bullen, *Seismological Tables*, 50 pp., British Association for the Advancement of Science, Gray-Milne Trust, London, 1958.
Kanamori, H., Mantle beneath the Japanese arc, *Phys. Earth Planet. Interiors*, *3*, 475, 1970.
Karig, D. E., Ridges and basins of the Tonga-Kermadec island arc system, *J. Geophys. Res.*, *75*, 239, 1970.
Katsumata, M., The effect of seismic zones upon the transmission of seismic waves (in Japanese), *Kenshin Ziho*, *25*, 19, 1960.
Katsumata, M., and L. R. Sykes, Seismicity and tectonics of the western Pacific: Izu-Mariana-Caroline and Ryukyu-Taiwan regions, *J. Geophys. Res.*, *74*, 5923, 1969.
McKenzie, D. P., Speculations on the consequences and causes of plate motions, *Geophys. J.*, *18*, 1, 1969.
Mitronovas, W., Seismic velocity anomalies in the upper mantle beneath the Tonga-Kermadec arc, Ph.D. thesis, Faculty of Pure Science, Columbia University, New York, 1969.
Mitronovas, W., B. Isacks, and L. Seeber, Earthquake locations and seismic wave propagation in the upper 250 km of the Tonga island arc, *Bull. Seismol. Soc. Amer.*, *59*, 1115, 1969.
Molnar, P., and J. Oliver, Lateral variations of attenuation in the upper mantle and discontinuities in the lithosphere, *J. Geophys. Res.*, *74*, 2648, 1969.
Oliver, J., and B. Isacks, Deep earthquake zones, anomalous structures in the upper mantle, and the lithosphere, *J. Geophys. Res.*, *72*, 4259, 1967.
Sattlegger, J., Series for three-dimensional migration in reflection seismic interpretation, *Geophys. Prosp.*, *12*, 115, 1964.
Sattlegger, J., Three-dimensional seismic depth computation using space-sampled velocity logs, *Geophysics*, *34*, 7, 1969.
Sykes, L. R., The seismicity and deep structure of island arcs, *J. Geophys. Res.*, *71*, 2981, 1966.
Sykes, L. R., B. Isacks, and J. Oliver, Spatial distribution of deep and shallow earthquakes of small magnitudes in the Fiji-Tonga region, *Bull. Seismol. Soc. Amer.*, *59*, 1093, 1969.
Utsu, T., Anomalies in seismic wave velocity and attenuation associated with a deep earthquake zone, 1, *J. Fac. Sci. Hokkaido Univ., Japan, Series VII (Geophys.)*, *3*, 1–25, 1967.

(Received May 20, 1970.)

Unclassified

Security Classification

DOCUMENT CONTROL DATA - R&D

(Security classification of title, body of abstract and indexing annotation must be entered when the overall report is classified)

1. ORIGINATING ACTIVITY *(Corporate author)*

LAMONT-DOHERTY GEOLOGICAL OBSERVATORY OF COLUMBIA UNIVERSITY, PALISADES, NEW YORK 10964

2a. REPORT SECURITY CLASSIFICATION

Unclassified

2b. GROUP

3. REPORT TITLE

THREE-DIMENSIONAL SEISMIC RAY TRACING IN A LATERALLY HETEROGENEOUS SPHERICAL EARTH

4. DESCRIPTIVE NOTES *(Type of report and inclusive dates)*

Scientific, Interim

5. AUTHOR(S) *(Last name, first name, initial)*

Klaus H. Jacob

6. REPORT DATE	7a. TOTAL NO. OF PAGES	7b. NO. OF REFS
January 4, 1971	15	23

8a. CONTRACT OR GRANT NO.

F19628-68-C-0341 APRA Order 292

b. PROJECT NO.

Project, Task, Work Unit Nos.

c. 8652-01-01

Dod Element 62701 D

d. Dod Subelement n/a

9a. ORIGINATOR'S REPORT NUMBER(S)

L.D.G.O. No. 1580

Scientific Report No. 13

9b. OTHER REPORT NO(S) *(Any other numbers that may be assigned this report)*

AFCRL-71- 0009

10. AVAILABILITY/LIMITATION NOTICES

1. This document has been approved for public release and sale; its distribution is unlimited.

11. SUPPLEMENTARY NOTES Reprinted from the Journal of Geophysical Research, Vol. 75, No. 32, November 10, 1970, pages 6675-6689.

12. SPONSORING MILITARY ACTIVITY

Air Force Cambridge Research Laboratories (LW)

L. G. Hanscom Field

Bedford, Massachusetts 01730

13. ABSTRACT

Recent seismological studies suggest lateral inhomogeneities in P and S velocities of the mantle that are associated with slabs of mobile lithosphere descending into the mantle beneath island arcs. In special cases, travel times of P traversing such zones can differ by as much as 5 sec and of S by up to 10 sec from standard travel times. In addition, such zones are characterized by relatively low attenuation of S-wave energy compared with high attenuation in a broad zone on the landward side of the active volcanoes. To explain the observed anomalous travel times and attenuation phenomena, it is necessary to trace the path of body waves through laterally heterogeneous earth models. The technique of ray tracing developed here uses Fermat's principle to obtain the differential equation of a ray in spherical coordinates. The position, direction, and travel time of the seismic wave front at any point along the curved ray path are obtained by numerical integration of the differential equation for an assumed three-dimensional, continuous velocity distribution. The problem of representing a realistic three-dimensional velocity structure in the earth is solved in a way that is especially suitable for use on computers. Some examples for rays traversing an island-arc structure are presented. The implications of this method of tracing rays in a laterally heterogeneous earth are discussed with respect to seismic travel-time studies, interpretation of residuals in terms of tectonic heterogeneities, source bias, and the precise location of earthquakes and nuclear explosions. $dT/d\Delta$ measurements from large seismic arrays and their inversion to obtain details of the velocity structure in the upper mantle are also discussed.

DD FORM 1 JAN 64 1473

Unclassified

Security Classification

14. KEY WORDS	LINK A		LINK B		LINK C	
	ROLE	WT	ROLE	WT	ROLE	WT
Three-dimensional seismic ray tracing Heteregeneous spherical earth						

INSTRUCTIONS

1. ORIGINATING ACTIVITY: Enter the name and address of the contractor, subcontractor, grantee, Department of Defense activity or other organization *(corporate author)* issuing the report.

2a. REPORT SECURITY CLASSIFICATION: Enter the overall security classification of the report. Indicate whether "Restricted Data" is included. Marking is to be in accordance with appropriate security regulations.

2b. GROUP: Automatic downgrading is specified in DoD Directive 5200.10 and Armed Forces Industrial Manual. Enter the group number. Also, when applicable, show that optional markings have been used for Group 3 and Group 4 as authorized.

3. REPORT TITLE: Enter the complete report title in all capital letters. Titles in all cases should be unclassified. If a meaningful title cannot be selected without classification, show title classification in all capitals in parenthesis immediately following the title.

4. DESCRIPTIVE NOTES: If appropriate, enter the type of report, e.g., interim, progress, summary, annual, or final. Give the inclusive dates when a specific reporting period is covered.

5. AUTHOR(S): Enter the name(s) of author(s) as shown on or in the report. Enter last name, first name, middle initial. If military, show rank and branch of service. The name of the principal author is an absolute minimum requirement.

6. REPORT DATE: Enter the date of the report as day, month, year; or month, year. If more than one date appears on the report, use date of publication.

7a. TOTAL NUMBER OF PAGES: The total page count should follow normal pagination procedures, i.e., enter the number of pages containing information.

7b. NUMBER OF REFERENCES: Enter the total number of references cited in the report.

8a. CONTRACT OR GRANT NUMBER: If appropriate, enter the applicable number of the contract or grant under which the report was written.

8b, 8c, & 8d. PROJECT NUMBER: Enter the appropriate military department identification, such as project number, subproject number, system numbers, task number, etc.

9a. ORIGINATOR'S REPORT NUMBER(S): Enter the official report number by which the document will be identified and controlled by the originating activity. This number must be unique to this report.

9b. OTHER REPORT NUMBER(S): If the report has been assigned any other report numbers *(either by the originator or by the sponsor)*, also enter this number(s).

10. AVAILABILITY/LIMITATION NOTICES: Enter any limitations on further dissemination of the report, other than those imposed by security classification, using standard statements such as:

(1) "Qualified requesters may obtain copies of this report from DDC."

(2) "Foreign announcement and dissemination of this report by DDC is not authorized."

(3) "U. S. Government agencies may obtain copies of this report directly from DDC. Other qualified DDC users shall request through

_____."

(4) "U. S. military agencies may obtain copies of this report directly from DDC. Other qualified users shall request through

_____."

(5) "All distribution of this report is controlled. Qualified DDC users shall request through

_____."

If the report has been furnished to the Office of Technical Services, Department of Commerce, for sale to the public, indicate this fact and enter the price, if known.

11. SUPPLEMENTARY NOTES: Use for additional explanatory notes.

12. SPONSORING MILITARY ACTIVITY: Enter the name of the departmental project office or laboratory sponsoring *(paying for)* the research and development. Include address.

13. ABSTRACT: Enter an abstract giving a brief and factual summary of the document indicative of the report, even though it may also appear elsewhere in the body of the technical report. If additional space is required, a continuation sheet shall be attached.

It is highly desirable that the abstract of classified reports be unclassified. Each paragraph of the abstract shall end with an indication of the military security classification of the information in the paragraph, represented as *(TS)*, *(S)*, *(C)*, or *(U)*.

There is no limitation on the length of the abstract. However, the suggested length is from 150 to 225 words.

14. KEY WORDS: Key words are technically meaningful terms or short phrases that characterize a report and may be used as index entries for cataloging the report. Key words must be selected so that no security classification is required. Identifiers, such as equipment model designation, trade name, military project code name, geographic location, may be used as key words but will be followed by an indication of technical context. The assignment of links, rules, and weights is optional.